14. S. M. Stanley, L. A. Hardie, *Palaeogeogr. Palaeoclimatol. Palaeoecol.* **144**, 3 (1998).
15. J. W. Morse, M. L. Bender, *Chem. Geol.* **82**, 265 (1990).
16. E. A. Burton, *Chem. Geol.* **105**, 163 (1993).
17. G. Hartley, A. Mucci, *Geochim. Cosmochim. Acta* **60**, 315 (1996).
18. J. W. Morse, Q. Y. Wang, *Geology* **25**, 85 (1997).
19. The sources of data for Fig. 1 are as follows: echinoderm data, composition, and temperature are from echinoid coronal plates from (*31*, *32*) and 24 crinoids from (*31*). Much chemical data exists for Mg-calcite cements, but few workers record temperature. The following have done so, and their data are used in Fig. 1 (*20–30*).
20. J. D. Milliman, J. Müller, *Sedimentology* **20**, 29 (1973).
21. R. N. Ginsburg, J. H. Schroeder, *Sedimentology.* **20**, 575 (1973).
22. T. Alexandersson, *J. Sediment. Petrol.* **44**, 7 (1974).
23. J. Müller, F. Fabricus, *IAS Spec. Publ.* **1** 235 (1974).
24. N. P. James, R. N. Ginsburg, D. S. Marszalek, P. W. Choquette, *Sediment. Petrol.* **46**, 523 (1976).
25. I. G. MacIntyre, *Sediment. Petrol.* **47**, 503 (1977).
26. W. Schlager, N. P. James, *Sedimentology* **25**, 67 (1978).
27. J. A. McKenzie, D. Bernoulli, *Tectonophysics*, **86** 149 (1982).
28. J. D. Pigott, L. S. Land, *Mar. Chem.* **19**, 355 (1986).
29. J. E. Andrews, *Scott. J. Geol.* **24**, 233 (1988).
30. S. J. Carpenter *et al.*, *Geochim. Cosmochim. Acta* **55**, (1991).
31. J. N. Weber, *J. Geol.* **81**, 543 (1973).
32. K. E. Chave, *J. Geol.* **62**, 266 (1954).
33. J. A. D. Dickson, *Nature* **105**, 587 (1965).
34. ———, *J. Sediment. Res.* **71**, 764 (2001).
35. ———, *Geochim. Cosmochim. Acta* **65**, 443 (2001).
36. Elemental concentrations were analyzed with a CAMECA SX50 electron microprobe (energy dispersive analysis); accelerating potential was 20 kV and beam current was between 3 and 5 nA, with a beam diameter of 5 to 8 μm. Analyses were conducted on 10 isolated spots on the echinoderm stereome. The location of analysis spots was checked after analysis by observing circular discoloration marks; the analyses from spots that were misplaced were rejected.
37. J. D. Rimstidt, A. Balog, J. Webb, *Geochim. Cosmochim. Acta* **62**, 1851 (1998).
38. J. W. Morse, M. L. Bender, *Chem. Geol.* **82**, 265 (1990).
39. P. A. Wilson, R. D. Norris, M. J. Cooper, *Geology* **30**, 607 (2002).
40. N. P. James, C. F. Klappa, *J. Sediment. Petrol.* **53**, 1051 (1983).

41. Thanks are due to A. Smith, S. Marcus, E. Harper, N. Butterfield, A. Molineux, P. Jell, D. Erwin, and J. Wendt for providing specimens for this study and to S. De Villiers and S. Bishop for discussion. S. Reed assisted with the electron microprobe analysis.

Supporting Online Material
www.sciencemag.org/cgi/content/full/298/5596/1222/DC1
Materials and Methods

9 July 2002; accepted 9 October 2002

Spatial and Temporal Offsets Between Proxy Records in a Sediment Drift

Nao Ohkouchi,[1]* Timothy I. Eglinton,[1]† Lloyd D. Keigwin,[2] John M. Hayes[2]

Chronologies for Late Quaternary marine sediment records are usually based on radiocarbon ages of planktonic foraminifera. Signals carried by other sedimentary components measured in parallel can provide complementary paleoclimate information. A key premise is that microfossils and other indicators within a given sediment horizon are of equal age. We show here that haptophyte-derived alkenones isolated from Bermuda Rise drift sediments are up to 7000 years older than coexisting planktonic foraminifera. This temporal offset, which is apparently due to lateral transport of alkenones on fine-grained particles from the Nova Scotian margin, markedly influences molecular estimates of sea surface temperatures. More broadly, the observation raises questions about both the temporal and the geographic fidelity of paleoenvironmental records encoded by readily transported components of sediments.

The development of multiple parallel proxy records derived from measurements of various sedimentary components is now commonplace for reconstruction of past changes in the ocean and climate. For example, the molecular sea surface temperature (SST) proxy $U^{K'}_{37}$ (*1–3*) complements information derived from the assemblages and oxygen isotopic ($\delta^{18}O$) compositions of planktonic foraminifera (*4*). A requirement for the successful coupling of molecular and microfossil-based proxies is that they reflect water column conditions at the same time. Bioturbation can, however, mix particles with differing ages (*5*). Resuspension and lateral advection of fine particles, which lead to the formation of sediment drifts (*6*), mix vertically sinking (autochthonous) and horizontally drifting (allochthonous) particles, potentially inducing the same net effect. Where allochthonous inputs are substantial, paleoclimate proxies associated with fine particles can be chronologically and spatially decoupled from those associated with coarser particles (*7*). The problem is important because sediment drifts, in which a meter of depth may represent only 1000 years, are often targeted for studies of abrupt climate change (*8*, *9*).

Drift sediments on the Bermuda Rise have been investigated in detail (*7–11*). Prior radiocarbon data, as well as analyses of planktonic foraminifera (*Globigerinoides ruber*) conducted as part of this study, indicate deposition rates of 12 to 24 cm per thousand years (ky) during the past 1200 calendar years and ~160 cm/ky from 17,000 to 23,000 calendar years before the present (yr B.P.) (Table 1) (cm/ky = cm per 1000 calendar years) (*8*, *10*, *12*). Table 1 also summarizes measured radiocarbon ages for total organic carbon (TOC), alkenones, and inorganic carbon in the fine fraction (FFIC) (particles <63 μm in diameter) from sediment intervals in three different cores (*13*). The first seven entries represent samples of Holocene age from a single box core. The average interval between samples is ~200 years. The remaining entries represent sediments deposited during the late glacial and deglaciation, 16 to 24 thousand years ago. The temporal resolution in this series is significantly lower, with an average interval between samples of about 1300 years. In all samples, the radiocarbon ages of the alkenones, TOC, and fine carbonates significantly exceed those of the planktonic forams. For the alkenones, the average difference is 4200 ^{14}C years. The TOC and FFIC are on average >5000 ^{14}C years older than the forams.

The foram ages provide the most accurate indication of the age of each sediment horizon. Relative to other sedimentary components, forams are large (>150 μm) and dense. These sand-sized particles settle rapidly from the overlying surface waters (*14*). Although bioturbation can in some cases mix forams of different ages with one another (*5*), the high sediment accumulation rates at the Bermuda Rise minimize potential offsets due to this process (*15*). In support of this idea, measurements on another planktonic foram, *Globorotalia inflata* (*16*), from the same samples yielded ages that were identical, within uncertainties, to those of *G. ruber*. Finally, the presence of bomb ^{14}C in forams in the shallowest depth interval (Table 1) provides clear evidence of prompt deposition.

The above differences in radiocarbon age provide compelling evidence that a significant portion of the carbon in the alkenones, TOC, and fine carbonates is derived from some source other than surface waters overlying the

---

[1]Department of Marine Chemistry and Geochemistry, [2]Department of Geology and Geophysics, Woods Hole Oceanographic Institution, Woods Hole, MA 02543, USA.

*Present address: Institute for Frontier Research on Earth Evolution, 2-15 Natsushima-cho, Yokosuka 237-0061, Japan.

†To whom correspondence should be addressed. E-mail: teglinton@whoi.edu

Bermuda Rise at the time of deposition. Any carbon-containing product formed at the same time and place as the forams would have exactly the same radiocarbon age [computations include corrections for isotopic fractionations (*17*)]. If the age difference were identical to the half-life of ^{14}C (5730 years), it could mean that, at the time of deposition, half of the alkenones delivered to the sediment were radiocarbon-dead (older than 50,000 years), with the other half being identical in age to the forams. Alternatively, it could mean that all of the alkenones delivered to the sediment had been synthesized 5730 years before their ultimate immobilization at this site. Intermediate cases, with smaller proportions of alkenones pre-aged for more than 5730 years, are also possible. In any case, the age differences require large allochthonous contributions, often exceeding 50%.

The magnitudes of the age discrepancies are highly variable. The standard deviations of the age-difference populations are ≈1600 years, indicating that a range of greater than ±3000 years would be required to include 95% of the observations and showing that the process responsible for delivering the allochthonous materials must be quite variable. These variations, possibly resulting from changes in provenance and modes of transport, could modulate the amount and/or the age of the allochthonous component.

On the Bermuda Rise, high rates of sedimentation are maintained by lateral advection and focusing of distal fine-grained sediments that are believed to derive predominantly from the Canadian margin off Nova Scotia (*10*, *18*, *19*). Sediments may be delivered from the margin by scouring and entrainment in the deep recirculating gyres (*20*, *21*) or by turbidity currents ("benthic storms") triggered by atmospheric or tectonic forcing or by sea-level change (*22*, *23*). In sediment drifts of the western North Atlantic, the resulting dilution of local materials by terrigenous debris is strongly anticorrelated with the abundance of carbonate minerals. On the Bermuda Rise, for example, concentrations of $CaCO_3$ range between 5 and 45% (*8*), indicating maximal and minimal dilution of autochthonous material, respectively.

Varying dilutions of carbonate, with concentrations ranging from 14 to 34%, are found in the Holocene samples examined in the present work (Fig. 1). The pronounced decrease in the abundance of carbonate during this interval is associated with a visible reddening of the sediment, indicating the presence of greater concentrations of hematite from the Canadian maritime provinces (*24*, *25*) and, based on excess ^{230}Th data, an abrupt and brief increase in sediment accumulation rate to values approaching 100 cm/ky (*26*). The decline in percent of $CaCO_3$ (% $CaCO_3$) is also associated with increased age offsets in all three fine-fraction carbon pools and with a decrease in $U^{K'}_{37}$, the alkenone-based SST proxy (Fig. 1). These convergent lines of evidence strongly suggest that sediment drifting, which delivers the diluent that expands the record, also supplies fine-grained carbonates, alkenones, and organic carbon that are associated with advected particles (*27*).

The analyses of the alkenones are of particular importance. These molecules are produced by haptophyte algae, notably the coccolithophorid *Emiliania huxleyi* (*2*). They are indubitably of marine origin. The age offsets cannot, therefore, be ascribed to terrigenous

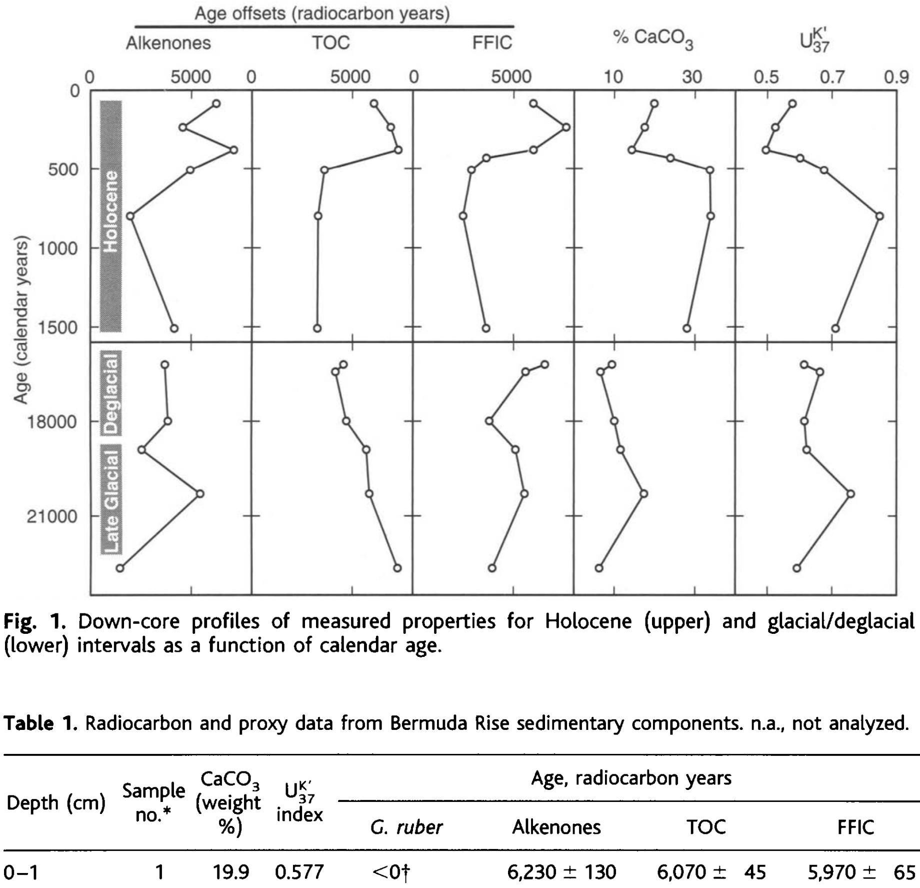

Fig. 1. Down-core profiles of measured properties for Holocene (upper) and glacial/deglacial (lower) intervals as a function of calendar age.

Table 1. Radiocarbon and proxy data from Bermuda Rise sedimentary components. n.a., not analyzed.

Depth (cm)	Sample no.*	$CaCO_3$ (weight %)	$U^{K'}_{37}$ index	Age, radiocarbon years				Age, calendar years		Initial $\Delta^{14}C$ (‰)			
				G. ruber	Alkenones	TOC	FFIC	Calibrated	Model	DIC	Alkenones	TOC	FFIC
0–1	1	19.9	0.577	<0†	6,230 ± 130	6,070 ± 45	5,970 ± 65		85	−42	−535	−525	−520
1–2	2	17.5	0.524	500 ± 25	5,060 ± 180	7,400 ± 55	8,100 ± 45	235	235	−33	−452	−590	−625
2–3	3	14.3	0.495	715 ± 30	7,810 ± 120	7,990 ± 60	6,690 ± 50	424	380	−38	−604	−613	−545
3–4	4	23.9	0.601	735 ± 35	n.a. n.a.	5,900 ± 55	4,410 ± 45	438	432	−40	n.a.	−495	−391
4–6	5	33.7	0.675	850 ± 30	5,780 ± 130	4,450 ± 55	3,750 ± 35	509	509	−44	−482	−389	−333
9–11	6	33.9	0.848	1,150 ± 25	3,100 ± 95	4,430 ± 50	3,640 ± 40	728	800	−54	−251	−365	−300
21–23	7	28.0	0.711	1,970 ± 45	6,130 ± 45	5,220 ± 90	5,610 ± 55	1,567	1,510	−53	−440	−373	−403
192–206	8	9.4	0.614	13,950 ± 65	17,650 ± 320	18,500 ± 110	20,500 ± 90	16,214	16,214	250	−210	−289	−446
282–292	9	10.0	0.615	15,700 ± 70	19,550 ± 430	20,400 ± 100	19,500 ± 85	18,228	18,000	279	−226	−304	−221
350–360	10	11.6	0.622	15,900 ± 300	18,450 ± 200	21,600 ± 80	21,000 ± 95	18,458	18,900	294	−10	−331	−280
345–355	11	6.6	0.663	14,150 ± 65	n.a. n.a.	18,300 ± 80	19,750 ± 120	16,444	16,444	254	n.a.	−251	−375
907–912	12	17.4	0.759	16,550 ± 140	22,000 ± 330	22,400 ± 95	22,100 ± 120	19,206	20,298‡	317	−247	−283	−256
1244–1260	13	6.3	0.592	19,550 ± 120	21,000 ± 650	26,800 ± 140	23,500 ± 120	22,658	22,658	357	135	−449	−169

*All samples are from adjacent cores on the Bermuda Rise. Samples 1 to 7 are from core OCE326-BC9 (33°41.6′N, 57°36.7′W, 4517 m water depth). Samples 8 to 10 are from core OCE326-GGC5 (33°41.5′N, 57°34.5′W, 4550 m water depth). Samples 11 to 13 are from core KNR31-GPC5 (33°41.2′N, 57°36.9′W, 4583 m water depth). †Contained carbon from atmospheric testing of nuclear weapons. ‡Interpolated from ages of samples 11 and 13 and consistent with all nine additional radiocarbon ages observed by Keigwin and Jones (*8*, *10*) at depths between 350 and 1450 cm in this same core.

inputs. Based on the calibration of Prahl *et al.* (*2*), the change in $U^{K'}_{37}$ corresponds to a decrease in SST of more than 7°C. Application of a recent SST calibration for suspended particulate matter in the euphotic zone of the Sargasso Sea (*28*) results in a slightly smaller shift, but both calibrations yield an implausibly large apparent reduction in SST, which is much greater than that inferred from the records of foraminiferal $\delta^{18}O$, during the late Holocene (*24*).

Together, the correlated Holocene variations in alkenone age offset, % $CaCO_3$, and $U^{K'}_{37}$ suggest advective inputs of "old, cold" alkenones synthesized earlier in productive waters on the Scotian Margin. The magnitude of these inputs can be estimated from a $U^{K'}_{37}$-based mixing calculation. The expected annual mean $U^{K'}_{37}$ indices for alkenones produced in present-day surface waters on the Bermuda Rise and Laurentian Fan are around 0.8 and 0.4, respectively (*28*, *29*). Using these values as end members implies that, depending on the depth interval in question, between 0 and 75% of the alkenones in Bermuda Rise sediments are from such colder waters.

More than two sources are, however, indicated. Although Table 1 shows that the $U^{K'}_{37}$ maximum and minimum in the Holocene are associated respectively with the smallest and largest age offsets, the age offset does not drop to zero at the $U^{K'}_{37}$ maximum. Therefore, not all allochthonous inputs cause variations in $U^{K'}_{37}$, indicating that the imported alkenones are not exclusively derived from colder regions.

A second view of the overall pattern for Holocene samples is shown in Fig. 2, which reveals that initial depletions of ^{14}C in alkenones, TOC, and fine carbonates are all correlated with the most robust previously recognized indicator of dilution (*8*), namely % $CaCO_3$. If the correlation resulted from mixing of only two components, all of the points would be expected to lie along a single line and the deviations of the points from the line would reflect only analytical uncertainties. The scatter is in fact much larger. Accordingly, the correlation is best explained by mixing of materials from multiple sources that are similar but not identical.

The average age offset of the allochthonous components can be estimated from the low-carbonate end of the regression line shown in Fig. 2. We consider the endpoint at 5% $CaCO_3$ for two reasons. First, observations show clearly that there is a significant concentration (minimum 4 weight %) of carbonate minerals in the fine fraction and, indeed, that it is much older than in the coexisting forams (Table 1) (*7*). Second, the minimum concentration of carbonate observed in these cores, plausibly from an interval containing only transported material, is 5%. In that case, the initial depletion of ^{14}C in the allochthonous material is –670 per mil (‰), which corresponds to an age difference of about 9000 calendar years. The observed correlation would not accommodate an average initial depletion approaching –1000‰ and therefore indicates that the bulk of the allochthonous material is resuspended marine debris rather than material derived from the erosion of beds undisturbed for 50,000 years or more.

Carbonate-poor intervals in North Atlantic sediments are generally associated with cooler climate periods (*30*). Similarly, the marked decrease in percent of $CaCO_3$ and associated fluctuations evident in the Holocene samples (Fig. 1) are coincident with the most recent millennial-scale cold event, the Little Ice Age (LIA) (*24*, *31*). These observations imply a link between sediment delivery, proxy signatures, and climate variability. Changes in the vigor and location of the deep western boundary current (*8*) or elevated wind stress (*32*) are both plausible explanations for enhanced delivery of fine-grained sediments during the LIA.

Expressed in radiocarbon years, age offsets in the late glacial and deglacial portion of the record differ from those in the Holocene. For the alkenones, however, the shift to slightly lower age offsets (an average of 3400 radiocarbon years in the late glacial/deglacial versus 4800 in the Holocene) is an artifact of changing levels of ^{14}C in the atmosphere (*33*). When initial values of $\Delta^{14}C$ are calculated (*34*), the average depletion in alkenones relative to forams at the time of deposition in the Holocene is 417 ± 51‰, whereas that in the deglacial and late glacial is 411 ± 64‰. This consistent depletion indicates that the $U^{K'}_{37}$ proxy is subject to uncertainty throughout the record. However, correlations between $U^{K'}_{37}$ and the alkenone age offset vary with time. These records yield mirror images in the Holocene but are roughly congruent in the late glacial/deglacial (Fig. 1), presumably reflecting a significant shift in the provenance of the transported alkenones. In contrast, the age offset for TOC trends consistently toward larger values in the pre-Holocene (Fig. 1), which is consistent with larger inputs of radiocarbon-dead terrigenous debris associated with glaciogenic sedimentation.

The evident sedimentological control of proxy records on the Bermuda Rise raises questions about the extent to which advected inputs have affected proxy records elsewhere. At this site, and presumably at other drifts, the parallel use of corresponding proxy records to infer aspects of past properties of the overlying surface ocean is prone to uncertainty. Evidence for advective control of alkenone SST records has been reported previously (*35*, *36*), and we have also observed significant age offsets (up to 4500 radiocarbon years) between alkenones and planktonic forams in another high-deposition-rate site on the Namibian margin (*37*). Such offsets may thus be a pervasive feature of depositional settings characterized by rapid sediment accumulation resulting from advection and focusing of fine particles.

Other sedimentary components that are used to develop down-core records and which reside in the fine fraction (such as nannofossils, clay particles, and pollen) may be similarly prone to allochthonous influences (*35*, *38*). The recognition and determination of the magnitude of offsets between proxies are particularly important where records of abrupt climate variability are sought from high-deposition-rate sites such as the Bermuda Rise. Measurements of the type reported here may also help to reconcile apparent contradictions between proxies. For example, sediment redistribution processes may be responsible for apparent leads and lags between proxy records (*39*). To this end, molecular-level ^{14}C measurements provide an important window into the age and provenance of organic compounds and other biogenic components residing in the fine fraction of Late Quaternary sediments.

Fig. 2. Initial depletions of ^{14}C relative to the surface reservoir versus % in samples of Holocene age. For example, Table 1 shows that at the time of their deposition, the alkenones in sample 7 were already depleted in ^{14}C by 387‰ [= –53 – (–440)] relative to DIC in surface waters. The depletions are significantly correlated with % $CaCO_3$ (r^2 = 0.75) and thus are consistent with dilution of a autochthonous component containing ~55% $CaCO_3$ by transported materials, which are on average 9000 years older and which contain ~5% $CaCO_3$. The differences between initial values of $\Delta^{14}C$ depend only on the radiocarbon analyses (*34*). The error bars are ±2 SD.

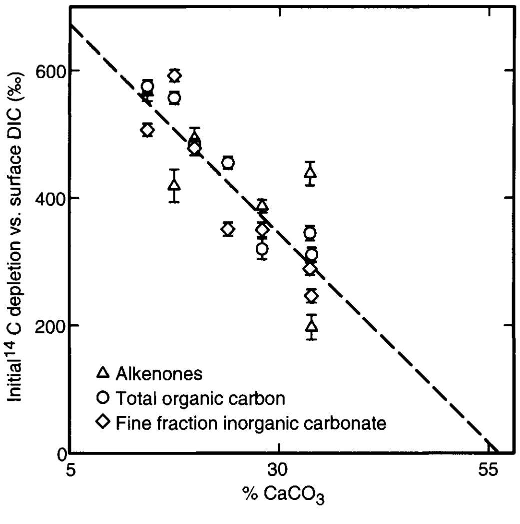

References and Notes

1. S. C. Brassell, G. Eglinton, I. T. Marlowe, U. Pflaumann, M. Sarnthein, *Nature* **320**, 129 (1986).
2. F. G. Prahl, L. A. Muehlhausen, D. L. Zahnle, *Geochim. Cosmochim. Acta* **52**, 2303 (1988).
3. $U^{K'}_{37} = [C_{37:2}]/([C_{37:2}] + [C_{37:3}])$, where $[C_{37:2}]$ and $[C_{37:3}]$ are concentrations of C_{37} alkadienone and alkatrienone, respectively (*2*).
4. F. Rostek *et al.*, *Nature* **364**, 319 (1993).
5. J.-C. Duplessy *et al.*, *Nature* **320**, 350 (1986).
6. I. N. McCave, *Philos. Trans. R. Soc. London Ser. B* **348**, 229 (1995).
7. L. D. Keigwin, B. H. Corliss, E. R. M. Druffel, E. P. Laine, *Quat. Res.* **22**, 383 (1984).
8. L. D. Keigwin, G. A. Jones, *J. Geophys. Res.* **99**, 12397 (1994).
9. J. P. Sachs, S. J. Lehman, *Science* **286**, 756 (1999).
10. L. D. Keigwin, G. A. Jones, *Deep-Sea Res.* **36**, 845 (1989).
11. J. F. Adkins, E. A. Boyle, L. D. Keigwin, E. Cortijo, *Nature* **390**, 154 (1997).
12. Standard techniques of calibration (*33*) were used to express the *G. ruber* ages in calendar yr B.P., assuming a constant reservoir age of 350 ± 40 calendar years for surface ocean dissolved inorganic carbon (DIC) at this site (*40*). Model ages were assigned based on these results and on prior observations (*7, 8, 10*).
13. The cores were correlated based on foraminiferal ^{14}C ages and % $CaCO_3$ profiles, as well as comparison with literature data (*10, 24*). For the ^{14}C measurements in core BC9, multiple subcores were correlated using % $CaCO_3$, and selected horizons were combined to yield sufficient alkenones for analysis. Alkenones were isolated as a compound class using a protocol described in detail by Ohkouchi *et al.* (*41*). Briefly, dried sediments were Soxhlet-extracted (ratio of methanol to dichloromethane, 3:7 v/v). The total lipid extract was saponified (using 0.5 M potassium hydroxide in methanol), and the neutral fraction was further separated into subfractions by silica gel column chromatography. A fraction containing alkenones was urea-adducted to separate straight chain compounds (including the alkenones) from branched and cyclic compounds. Polyunsaturated ketones were separated by argentation column chromatography, and a second silica gel column chromatographic step was used to remove remaining impurities. The resulting fraction contained only C_{36}-C_{39} alkenones with estimated purities consistently >95%. The purified alkenones were transferred to quartz tubes, vacuum-sealed with 100 mg of CuO, and combusted. The CO_2 produced was recovered and purified by cryogenic distillation and reduced to graphite over a cobalt catalyst (*42*). A small aliquot was used for measurement of $\delta^{13}C$. ^{14}C measurements were performed using methods for accurate determination of $^{14}C/^{12}C$ ratios in small samples at the National Ocean Science Accelerator Mass Spectrometry Facility (*43*).
14. L. Fok-Pun, P. D. Komar, *J. Foram. Res.* **13**, 60 (1983).
15. E. Bard, *Paleoceanography* **16**, 235 (2001).
16. N. Ohkouchi, T. I. Eglinton, unpublished data.
17. W. G. Mook, J. van der Plicht, *Radiocarbon* **41**, 227 (1999).
18. E. P. Laine, C. D. Hollister, *Mar. Geol.* **39**, 277 (1981).
19. D. O. Suman, M. P. Bacon, *Deep-Sea Res.* **36**, 869 (1989).
20. D. J. W. Piper, D. A. V. Stow, W. R. Normark, in *Submarine Fans and Related Turbidite Systems*, A. H. Bouma, W. R. Normark, N. E. Barnes, Eds. (Springer, New York, 1985), pp. 137–142.
21. W. J. Schmitz, M. S. McCartney, *Rev. Geophys.* **31**, 29 (1993).
22. W. D. Gardner, L. G. Sullivan, *Science* **213**, 329 (1981).
23. P. P. E. Weaver, R. G. Rothwell, J. Ebbing, D. Gunn, P. M. Hunter, *Mar. Geol.* **109**, 1 (1992).
24. L. D. Keigwin, *Science* **274**, 1504 (1996).
25. ——, R. S. Pickart, *Science* **286**, 520 (1999).
26. J. F. Adkins, E. A. Boyle, L. D. Keigwin, *Eos* **76**, 282 (1995).
27. R. G. Keil, E. Tsamakis, B. Fuh, C. Giddings, J. I. Hedges, *Geochim. Cosmochim. Acta* **58**, 879 (1994).
28. M. H. Conte, J. C. Weber, L. L. King, S. G. Wakeham, *Geochim. Cosmochim. Acta* **65**, 4275 (2001).
29. Ocean Climate Laboratory, *World Ocean Atlas, 1998* (National Oceanographic Data Center, Silver Spring, MD, 1999) [CD ROM].
30. W. L. Balsam, F. W. McCoy Jr., *Paleoceanography* **2**, 531 (1987).
31. R. S. Bradley, P. D. Jones, Eds., *Climate Since A.D. 1500* (Routledge, London, revised ed., 1995).
32. S. R. O'Brien *et al.*, *Science* **270**, 1962 (1995).
33. M. Stuiver, P. J. Reimer, T. F. Braziunas, *Radiocarbon* **40**, 1127 (1998).
34. Initial $\Delta^{14}C = (\Delta^{14}C_{meas} + 1)\exp(\lambda_P\tau) - 1$, where $\Delta^{14}C_{meas} = \exp(-\lambda_L t - \lambda_P\Delta t) - 1$; $\lambda_P = \ln 2/5730$ year^{-1}; $\lambda_L = \ln 2/5568$ year^{-1}; τ = time interval between deposition and measurement in calendar years (= model age + Δt, because model age refers to time before 1950); t = conventional radiocarbon age in radiocarbon years; and Δt = 51 calendar years, the time interval between 1950 and the measurement (*17*). Expression of $\Delta^{14}C$ in ‰ units implies multiplication by 1000.
35. P. P. E. Weaver *et al.*, *Paleoceanography* **14**, 336 (1999).
36. A. Benthein, P. J. Muller, *Deep-Sea Res. I* **47**, 2369 (2000).
37. G. Mollenhauer *et al.*, unpublished results.
38. G. M. Henderson, N. C. Slowey, *Nature* **404**, 61 (2000).
39. M. Ikehara *et al.*, *Geophys. Res. Lett.* **24**, 679 (1997).
40. E. R. M. Druffel, *Science* **275**, 1454 (1997).
41. N. Ohkouchi, L. Xu, C. M. Reddy, T. I. Eglinton, in preparation.
42. A. Pearson, A. P. McNichol, R. J. Schneider, K. F. von Reden, *Radiocarbon* **40**, 61 (1998).
43. K. F. von Reden, R. J. Schneider, A. P. McNichol, A. Pearson, *Radiocarbon* **40**, 247 (1998).

44. We thank J. McManus, J. Sachs, J. Adkins, and G. Eglinton, for discussions; three anonymous reviewers for constructive criticism of an earlier version of this manuscript; D. Montluçon, E. Roosen, and National Ocean Sciences Accelerator Mass Spectrometry Facility staff for laboratory assistance; and NSF (grant OCE-9809624) and the Japanese Society for the Promotion of Science for financial support. This is Woods Hole Oceanographic Institution contribution no. 10820.

20 June 2002; accepted 27 September 2002

10.1126/science.1075287
Include this information when citing this paper.

Vibrational Transition Moment Angles in Isolated Biomolecules: A Structural Tool

F. Dong and R. E. Miller

Infrared spectroscopy is used extensively in the study of isolated biomolecules, but it becomes less useful as it is applied to systems of increasing complexity. Even if the individual vibrational bands can be resolved spectroscopically, their assignment becomes problematic when they are more closely spaced than can be determined using ab initio methods. We describe a method that helps to alleviate this difficulty by measuring the direction of the vibrational transition moment for each vibrational band. The molecules of interest (adenine and cytosine) are cooled to 0.37 kelvin in liquid helium nanodroplets and oriented in a large dc electric field. A polarized infrared laser is then used to determine the directions of the infrared transition moments relative to the permanent dipole moment. Comparisons with ab initio calculations provide detailed structural information, including experimental evidence for nonplanarity of adenine and three tautomers of cytosine.

One reason for the recent interest in the spectroscopic study of isolated biomolecules (*1, 2*) is that these results can be compared with ab initio theory, providing new and important insights into the structure and dynamics of these systems. Noncovalent interactions, including the intramolecular forces between different parts of a highly flexible biomolecule (*3*) and intermolecular (solvent) interactions in clusters (*4*), are also being studied in this way. In the latter case, the issue of how the solvent influences the conformational preferences of the molecule can also be addressed by making comparisons between the structures observed for the isolated molecule and those in the associated water clusters of varying size (*5*); intermolecular hydrogen bonding interactions can often "strain" the molecule of interest into conformations that are not favorable for the isolated molecule (*6*).

Vibrational spectroscopy is used extensively in these studies, because it can provide detailed information on both the structure and dynamics of systems of modest complexity (*1, 4, 7, 8*). For larger systems that have multiple conformations, the problems associated with resolving and then assigning the observed vibrational bands become formidable. Although pump-probe methods have proven useful in separating spectra associated with different conformers (*7*), progress toward the study of more complex systems will ultimately be limited by the ability to assign the different vibrational bands.

Here, we discuss a method for measuring the direction of the transition moment for

---

Department of Chemistry, University of North Carolina, Chapel Hill, NC 27599, USA.